JOURNAL OF GEOPHYSICAL RESEARCH, VOL. 111, D23S22, doi:10.1029/2006JD007465, 2006

Structure and formation of the highly stable marine boundary layer over the Gulf of Maine

Wayne M. Angevine,[1,2] J. E. Hare,[1,2] C. W. Fairall,[3] Daniel E. Wolfe,[3] R. J. Hill,[1,2] W. A. Brewer,[3] and Allen B. White[1,2]

Received 2 May 2006; revised 26 July 2006; accepted 28 August 2006; published 21 November 2006.

[1] A shallow, stable boundary layer is ubiquitous over the cool waters of the Gulf of Maine in summer. This layer affects pollutant transport throughout the region by isolating overlying flow from the surface. In this paper, we explore how the stable boundary layer is formed and describe its characteristics. The temperature profile of the lowest 1–2 km of the atmosphere over the Gulf of Maine is remarkably similar regardless of transport time over water or the time of day when the flow left the land, provided only that the flow is offshore. This similarity is forced by the (roughly) constant water temperature and the (roughly) constant temperature of the free troposphere over the continent. However, the processes leading to the similar profiles are quite different depending on the time of day when the flow crosses the coast. Air leaving the coast at night already has a stable profile, whereas air leaving the coast at midday or afternoon has a deep mixed layer. In the latter case, the stable layer formation over the water is of interest. Using observations of surface fluxes, profiles, and winds on the NOAA Research Vessel *Ronald H. Brown* from the 2004 International Consortium for Atmospheric Research in Transport and Transformation (ICARTT)/New England Air Quality Study, we show that the formation of the stable layer, which involves cooling a roughly 50- to 100-m-deep layer by 5–15 K, occurs within 10 km and a half hour after leaving the coast. The internal boundary layer near shore is deeper than predicted by standard relationships. Historical data are explored and also show deeper internal boundary layers than predicted. We also describe one exceptional case where a 200-m-deep neutral layer was observed and discuss the degree of isolation of the stable boundary layer and its duration.

Citation: Angevine, W. M., J. E. Hare, C. W. Fairall, D. E. Wolfe, R. J. Hill, W. A. Brewer, and A. B. White (2006), Structure and formation of the highly stable marine boundary layer over the Gulf of Maine, *J. Geophys. Res.*, *111*, D23S22, doi:10.1029/2006JD007465.

1. Introduction

[2] The cool waters of the Gulf of Maine cause a shallow stable boundary layer to form in the summer whenever air flows from the adjacent land. Since the prevailing winds are westerly, these stable boundary layers are very common in summer. The structure of the boundary layer controls the transport of pollutants emitted on the continent. In particular, emissions from the urban corridor of the northeastern United States can be efficiently transported long distances [*Neuman et al.*, 2006]. Strong concentrations of urban-source pollution routinely reach the coast of Maine, hundreds of kilometers from concentrated sources. Transport as far as Europe in the lower atmosphere has been observed.

[3] Previous papers have described the basic structure of this boundary layer and its effects on pollutant transport. They emphasized observations [*Angevine et al.*, 2004] and mesoscale modeling [*Angevine et al.*, 2006]. The observations showed a remarkable degree of similarity of temperature profiles in the lower atmosphere over the Gulf of Maine, nearly regardless of the distance from shore, the transport time, or the time of day when the air left the coast. The key question left unresolved is this: How is the stable boundary layer formed? We will describe the processes that produce the observed profiles, as we have come to understand them from additional measurements and analysis. Our analysis is, unfortunately, not completely conclusive, because some useful measurements were not available, but we can describe many aspects of the question.

[4] In July and August 2004, the International Consortium for Atmospheric Research into Transport and Transformation (ICARTT) was the umbrella for a large-scale study in the northeastern United States, Canada, and the North Atlantic. The part of that study focused on regional air quality in northern New England (New Hampshire, Maine, and the Gulf of Maine) was called the New England Air Quality Study (NEAQS) 2004. The NOAA Research Vessel *Ronald*

[1] Cooperative Institute for Research in Environmental Sciences, University of Colorado, Boulder, Colorado, USA.
[2] Also at Earth System Research Laboratory, NOAA, Boulder, Colorado, USA.
[3] Earth System Research Laboratory, NOAA, Boulder, Colorado, USA.

0148-0227/06/2006JD007465$09.00

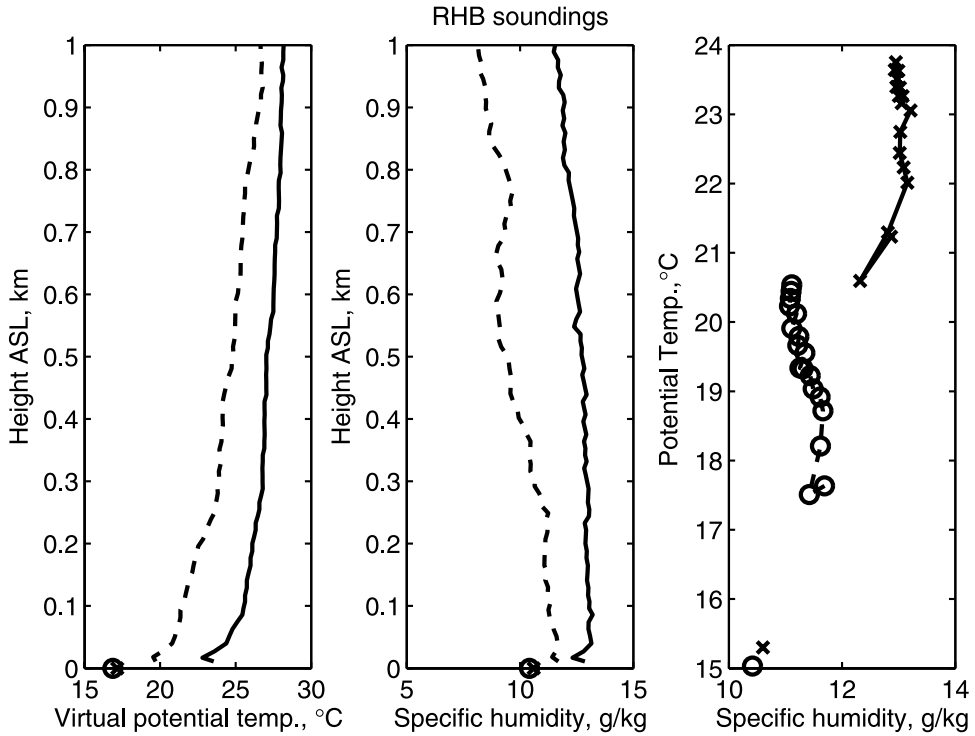

Figure 1. Soundings from the ship during the stationary period. Solid line and crosses are from sounding launched at 1800 LST 15 July, and dashed line and circles are from sounding launched at 0600 LST 16 July. (left) Virtual potential temperature, (middle) specific humidity, (right) and mixing diagrams. The sea surface temperature and (saturation) specific humidity are shown as circles. See text for discussion of mixing diagram.

H. Brown was a key component of NEAQS 2004. The ship was heavily instrumented for in situ measurements of gas-phase and aerosol atmospheric chemistry. Meteorological instrumentation included a Doppler lidar, a radar wind profiler, rawinsonde equipment, and a surface flux package. The flux package was the major addition since the NEAQS 2002 study described in our earlier papers. The measurements from the flux package and associated technical and scientific issues are discussed by *Fairall et al.* [2006].

[5] A few studies of warm airflow over cool water have appeared in the literature [*Atkinson et al.*, 2001; *Atkinson and Zhu*, 2005; *Brooks et al.*, 1999; *Brooks and Rogers*, 2000; *Craig*, 1946; *Emmons*, 1947; *Rogers et al.*, 1995; *Smedman et al.*, 1997a, 1997b; *Zhu and Atkinson*, 2005]. The air-sea temperature differences observed here are toward the larger end of those studied by other groups. *Smedman et al.* [1997b] included one case with similar conditions. The Craig paper is particularly interesting, showing a very wide range of conditions including some with strong air-sea temperature differences and short over-water fetch. Their aircraft soundings extended down to 20 feet (~6 m) ASL, a feat rarely attempted in more recent studies, but necessary to explore these very shallow internal boundary layers.

2. Investigating Stable BL Formation: 15–16 July

[6] The ship was nearly stationary approximately 10 km offshore from 2000 UTC 15 July until 1200 UTC 16 July. During these 16 hours, the near-surface wind started at SE and veered to SW where it remained for most of the period. The flow at the ship was from land throughout the period, although early in the period the flow may have only been over land a relatively short time.

[7] Figure 1 shows two soundings measured by rawinsondes launched from the ship. Virtual potential temperature, the correct quantity to describe static stability, is plotted, along with specific humidity. Both the evening and morning soundings show statically stable boundary layers. The sondes are launched from the deck of the ship, and therefore do not show the additional stable temperature difference that exists between the deck and the sea surface. The air temperature over land 10 km upwind of the ship differs by approximately 7–8° between the times of these two soundings.

[8] In Figure 2, micrometeorological measurements from the ship during the stationary period are plotted. Three distinct subperiods can be seen. First, from 1500 LST 15 July until 1900 LST 16 July, the sea surface is substantially (4–6 K) cooler than the air at 15 m. The wind at 15 m is 3–7 m s^{-1}. The sensible heat flux is very small, and the vertical velocity variance is moderate. The temperature reported by an operational surface site at Beverly, Massachusetts (42.58N, 70.92W, southwest of Cape Ann), is shown for comparison. On this particular afternoon, the boundary layer over land was probably not entirely well mixed and was topped by approximately ¾ cloud cover. Unfortunately no relevant soundings over land are available.

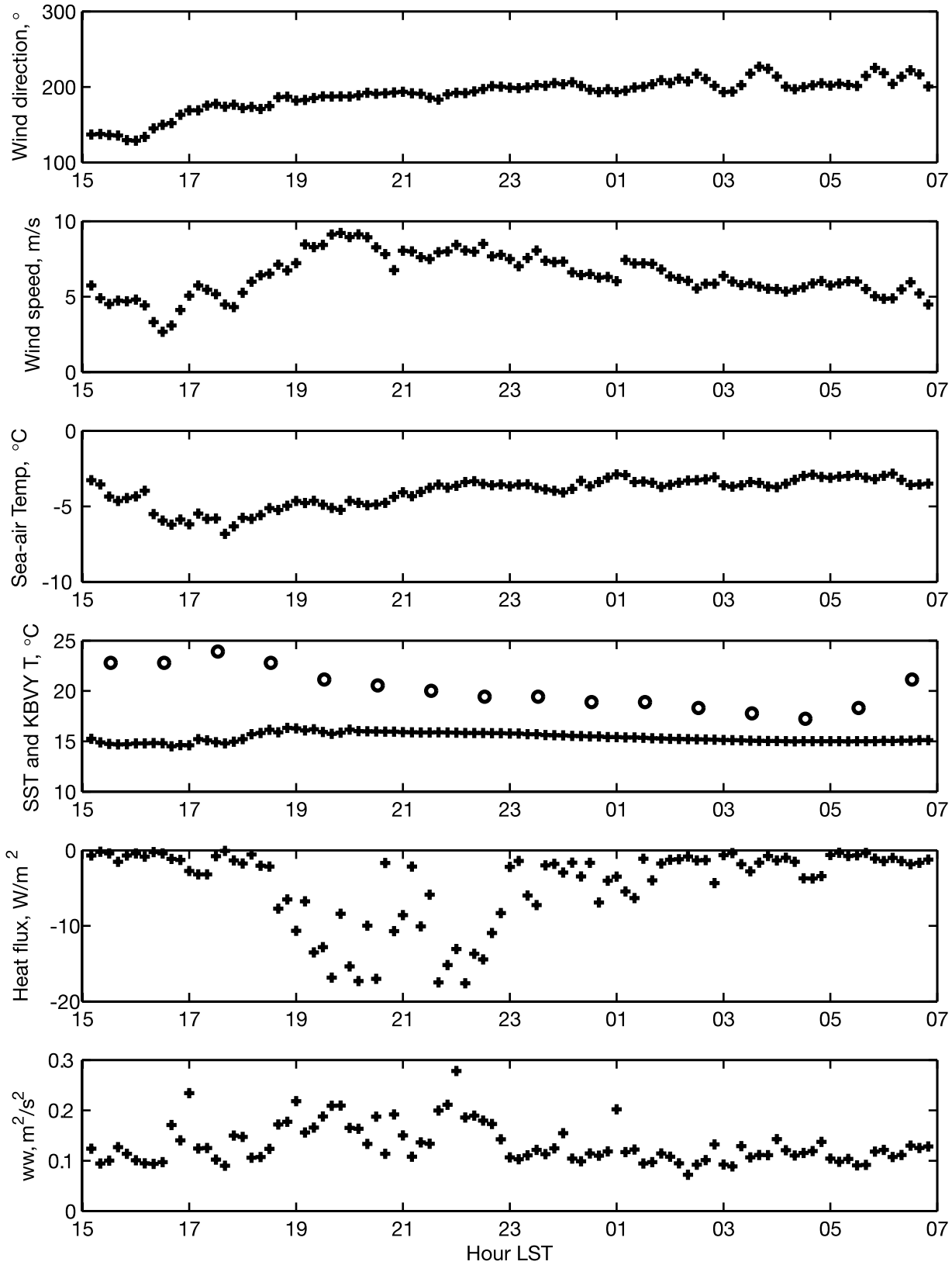

Figure 2. Micrometeorological measurements from the ship's flux package during the stationary period on 15–16 July. Temperature at Beverly, Massachusetts, also shown.

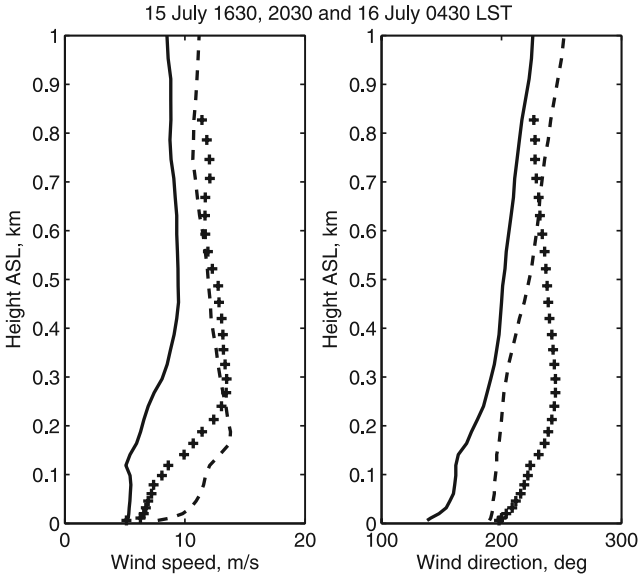

Figure 3. Wind profiles measured above the ship at 1630 LST 15 July (solid), 2030 LST 15 July (dashed), and 0430 LST 16 July (pluses). Profiles are 1-hour averages centered at the specified time, using lidar measurements up to about 500 m and wind profiler data above.

In the next period, from 1900 LST to 2300 LST, the sea-air temperature difference is less pronounced, the wind is stronger, the heat flux is larger in magnitude (more negative), and the turbulence intensity is decreasing, as is the air temperature over land. During this time, the boundary layer over land is cooling and becoming more stable, and its turbulence is decreasing. Finally, from 2300 LST to 0700 LST 16 July, the sea-air temperature difference holds steady at about −3 K, the wind speed decreases slowly, the heat flux is again very small, and the turbulence intensity is also small. This corresponds to a fully formed stable nocturnal boundary layer over the land. Toward the end of this period the air temperature over land begins to rise rapidly.

[9] A mixing diagram (potential temperature vs. specific humidity) is also shown for each sounding in Figure 1, including data below 200 m ASL. See [*Craig*, 1946] for a full discussion of this type of diagram. Samples of air in a layer that is undergoing or has undergone mixing with a surface having the same temperature and humidity as the local surface should fall along a straight line that points toward the local surface sample. This is a more sensitive indication of the depth of influence of the local surface than the virtual potential temperature sounding alone. Samples of air from a well-mixed layer will cluster about the same point on the diagram. The lowest point of each of the two soundings does not belong to the set, and has probably been affected by either prelaunch conditions or by the wake of the ship. Ignoring that lowest point, we can see a short mixing line in each sounding, extending up to approximately 40 m ASL.

[10] The most interesting thing about the flux observations is what we do not see: There is no period of large negative heat flux that would account for the cooling of the lowest few tens of meters of the temperature profile in the afternoon and evening, when the air over the land is warm. The winds measured at the ship are definitely offshore, so the column must be cooled before it reaches the ship. The transport time from shore, based on the surface wind measurements at the ship, is only about 20 min. Even during the period with the largest negative heat flux, that flux is only sufficient to cool a 40-m layer by 1–2 K during the transport. The observed cooling is approximately 7 K. We must conclude that the cooling is already nearly over before the air reaches the ship.

[11] Wind profiles above the ship are shown in Figure 3 (D. E. Wolfe et al., Shipboard multi-sensor merged wind profiles from NEAQS 2004: Radar wind profiler, high-resolution Doppler lidar, GPS rawinsonde, submitted to *Journal of Geophysical Research*, 2006). A 1-hour-averaged profile is shown from each of the subperiods mentioned above. These are chosen to be representative of the periods, not to correspond to the soundings in Figure 1, which were taken at scheduled times and therefore not necessarily at the most interesting times. In the first period (1630 LST profile) there is strong directional shear below 50 m and above 150 m. Later, in the 2030 LST profile, there is little directional shear in the low levels, but a very substantial increase in wind speed with increasing height. Finally, the 0430 LST profile again has a substantial directional shear between the surface and 250 m, and also a very strong increase in speed with height. Shear measures are shown hourly for the entire period in Figure 4. The times of the profiles in Figure 3 are marked with pluses in Figure 4. Directional shear in both layers (6–100 m and 6–500 m) is greatest in the early subperiod, when the air-sea temperature difference is large, surface wind speed low, heat flux small, and turbulence most intense. This early subperiod has, however, the smallest vector shear in the 6–100 m layer. The middle subperiod, with moderate air-sea temperature difference, stronger surface winds, larger (negative) heat flux, and decreasing turbulence intensity, has little directional shear and moderate vector shear in the 6–100 m layer. The vector shear then remains roughly constant while the directional shear in the 6–100 m layer increases for the later subperiod, when the air-sea temperature difference is small, surface wind speeds decreasing, and heat flux and turbulence intensity are small.

[12] The strong turning of the wind direction with height makes interpretation in terms of simple one-dimensional internal boundary layers (IBL) difficult. However, when the ship is close to shore, as in the 15–16 July case, IBL concepts may be useful. For the case of warm air advected a distance x over cold water, *Garratt* [1990] asserts that the IBL height h can be estimated by

$$h = 0.02U\left(\frac{g(\theta_v - \theta_{vs})}{\theta_v}\right)^{-1/2} x^{1/2} \quad (1)$$

where g is gravitational acceleration and θ_v and U are the atmospheric mixed layer properties over land that flow out onto the sea with surface virtual potential temperature θ_{vs}. For the conditions at 1800 LST 15 July ($\theta_v - \theta_{vs} \approx 7$ K and $U \approx 5$ m s^{-1}) equation (1) gives an IBL depth of 21 m at an overwater fetch of 10 km, 36 m at 30 km, and 66 m at 100 km. Since the observed IBL depth (∼40 m) is considerably greater

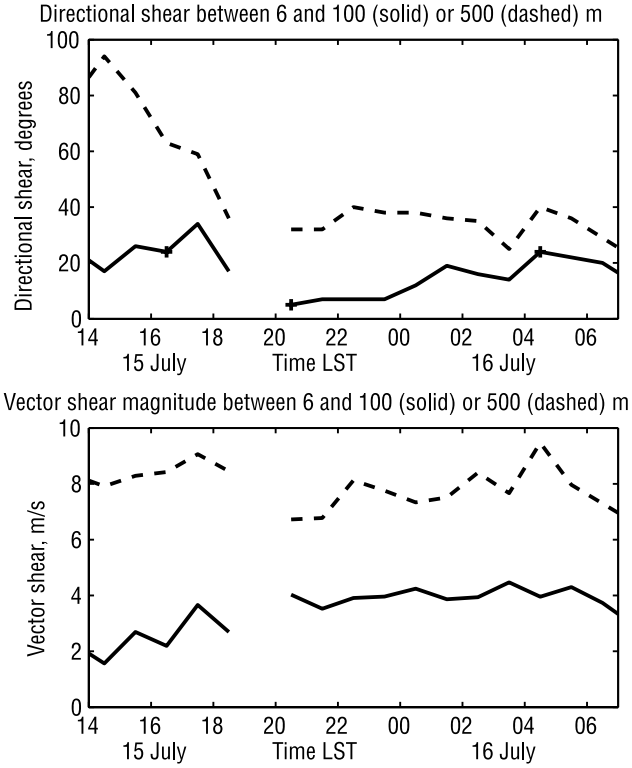

Figure 4. Two measures of wind shear above the ship starting at 1400 LST 15 July. Solid lines are shear between 6 m and 100 m, and dashed lines are shear between 6 m and 500 m. (top) Directional shear (difference in wind direction, upper level minus lower level) and (bottom) the magnitude of the shear vector.

at 10 km than this prediction, some process not accounted for in the derivation of (1) may be at work.

3. A Broader Range of Conditions: 30 July to 1 August

[13] For a broader perspective, we present measurements from the 3-day period 30 July to 1 August. During this time, the ship explored the Gulf of Maine between Cape Ann and midcoastal Maine, with some excursions farther offshore (Figure 5). The sea surface temperatures varied by as much as 7 K. At the surface, the flow was offshore from the southwest. Transport times from the coast to the ship were 3–12 hours, on the basis of surface wind speeds. Soundings during the period (Figures 6a and 6b) are again remarkably similar, with strong, shallow, surface-based statically stable layers. The mixing diagrams for data below 200 m show variable heights of local influence, ranging from 40 to 100 m. The surface-based stable layers are also approximately 50–100 m deep. The next layer above, the "intermediate layer," is also statically stable but much less so. In several soundings, more than one distinct layer can be seen below 1 km. Again, we note that the layer below the minimum height of the soundings is also statically stable, with sea-air temperature differences of 1–7 K (Figure 7). The micrometeorological measurements in Figure 7 show a range of wind speeds, turbulence intensities, and heat fluxes. The heat flux and vertical velocity variance are correlated with wind speed but not with the temperature difference. Heat flux magnitudes are in the range expected for well-developed stable boundary layers.

[14] Selected wind profiles from 30 July to 1 August are shown in Figure 8. The profiles are chosen to correspond as closely as possible to the sounding times shown in Figures 6a and 6b, but not all times have wind profile data available. Many of the profiles have pronounced low-level jets (wind speed maxima above the surface but below ~500 m). Such jets are ubiquitous in stable boundary layers, but the mechanisms contributing to their formation are still an active topic of research [*Chimonas*, 2005; *Lundquist*, 2003]. For our purposes, it is sufficient to note that the wind speed at or below 100 m may be substantially faster than at slightly higher levels. There is almost always some directional shear below 100 m, although in the middle part of the period it is relatively small. Directional shear between 6 m and 500 m is, as expected, larger than in the shallower layer. Because of the common jet structure, the vector shear (not shown) is sometimes less between 6 m and 500 m than between 6 m and 100 m.

4. Discussion and Conclusions

[15] We find that the stable boundary layer forms very quickly in flow off the land during the day, as shown at 1800 LST on 16 July. We see a temperature difference of 7 K between the sea surface and the air at 40 m. The transport time from land is only 20 min. Clearly the small local heat flux is insufficient to cool the layer so rapidly. To cool the layer by the measured amount in 20 min requires a heat flux of approximately -150 W m^{-2}. The observed profiles are strongly concave upward, that is, the surface layer is cooled much more than the rest of the new marine boundary layer.

[16] To explore the relationship between the prediction (1) of IBL height and measurements further, we have extracted relevant parameters from *Craig* [1946] and from the 30 July to 1 August ICARTT period discussed in section 3 above. From *Craig* [1946] we have selected cases with clearly defined stable internal boundary layers and for which we can be reasonably confident in the flow direction and distance from shore. These cases are presented in Table 1. The ICARTT data, including the cases discussed

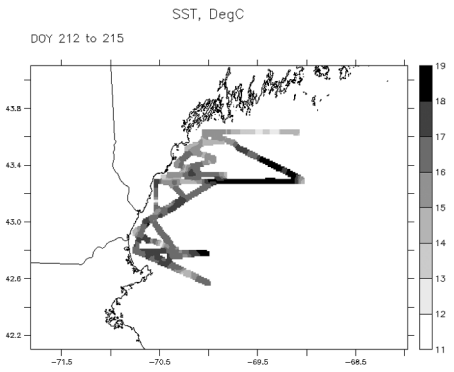

Figure 5. Sea surface temperature along the cruise tracks for 30 July to 1 August 2004.

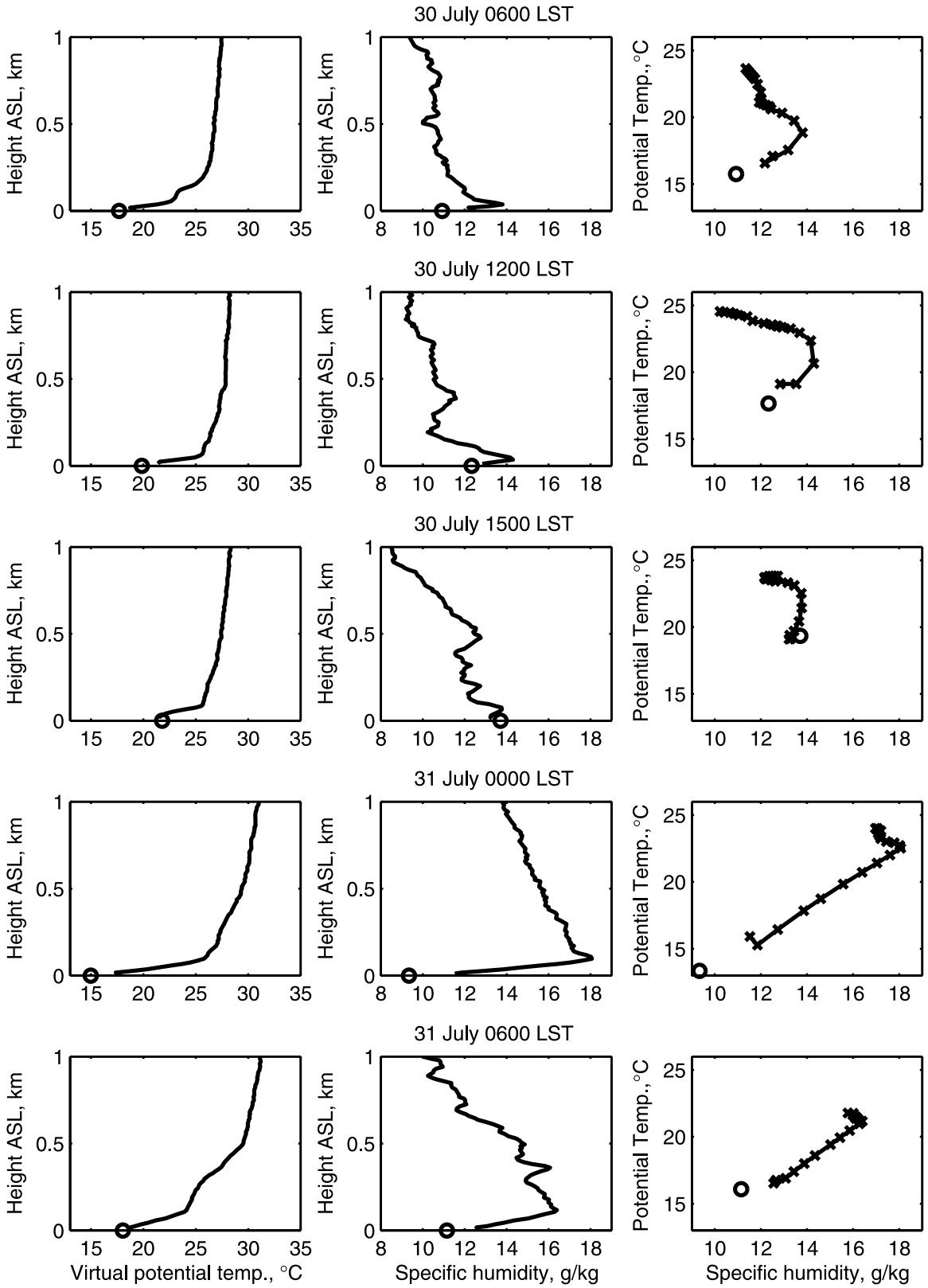

Figure 6a. Soundings from the ship on 30–31 July.

in sections 2 and 3 above, are presented in Table 2. Figure 9a shows a simple comparison of the predicted IBL height from (1) with the measured height for all the tabulated cases. Significant uncertainties are associated with these data, including but not limited to the difficulty of extracting precise numbers from the available graphics, possible ambiguities in determining the measured IBL height, the effects of changing sea surface temperature along the

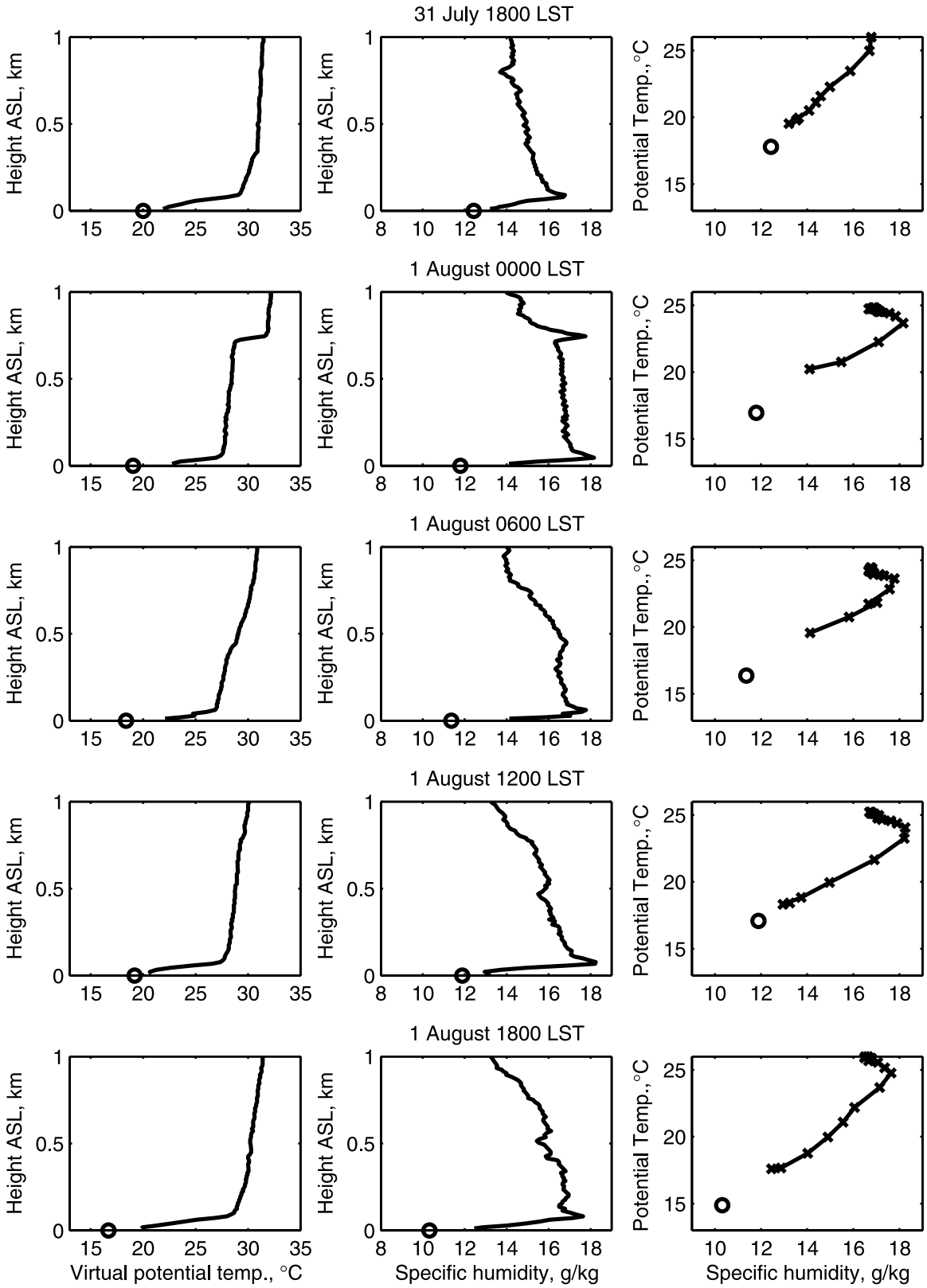

Figure 6b. Soundings from the ship on 31 July and 1 August.

trajectory, and the effects of directional wind shear. For the ICARTT data, the distance to shore is determined from a trajectory tool using observed ship and buoy data [*White et al.*, 2006]. There is significant uncertainty in determining the distance from shore, since the flow is nearly parallel to the coast for much of its trajectory in several cases. Given those uncertainties, we must be somewhat circumspect in our conclusions. However, we can say the following with

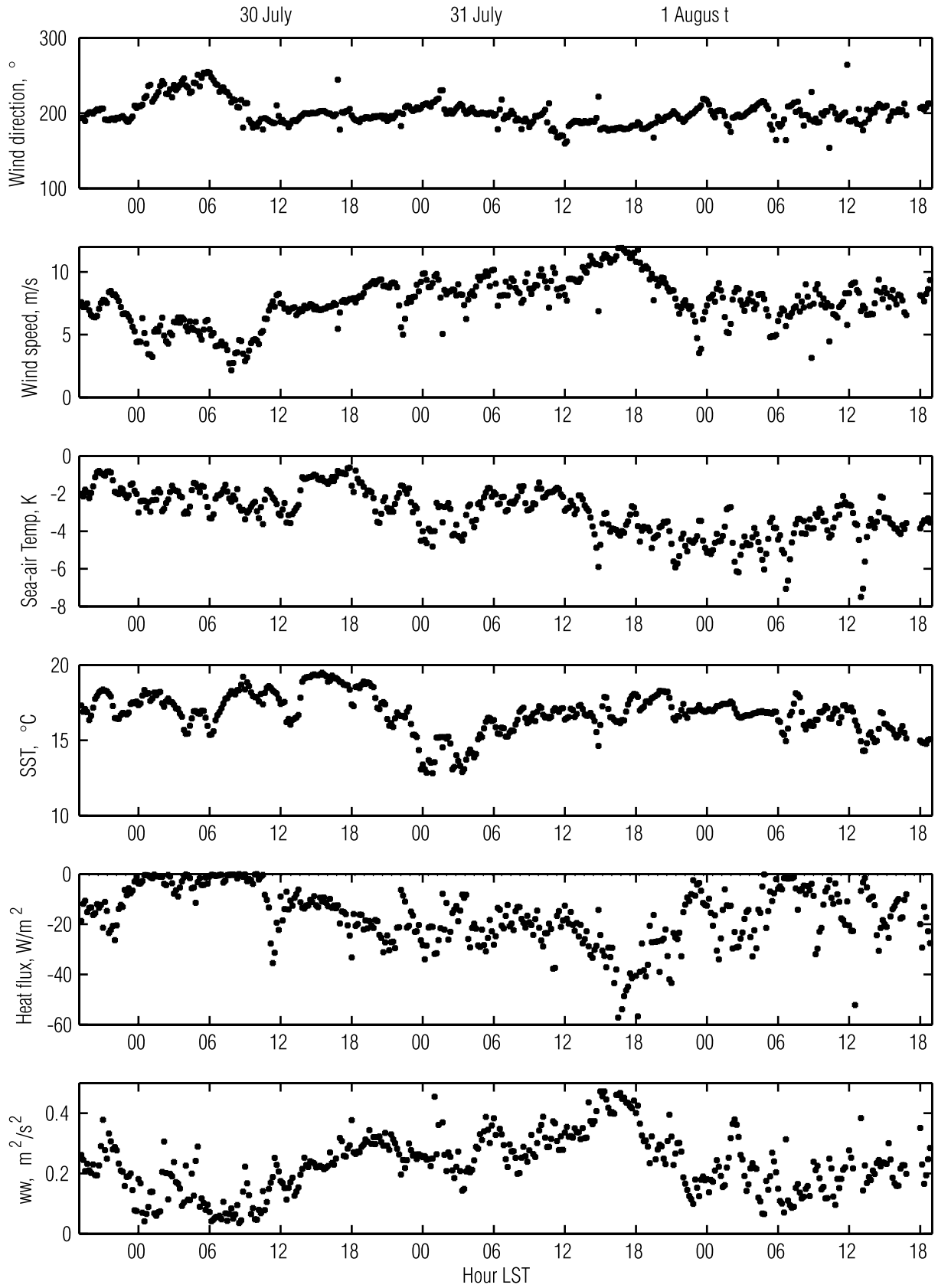

Figure 7. Micrometeorological measurements from the ship on 30 July to 1 August.

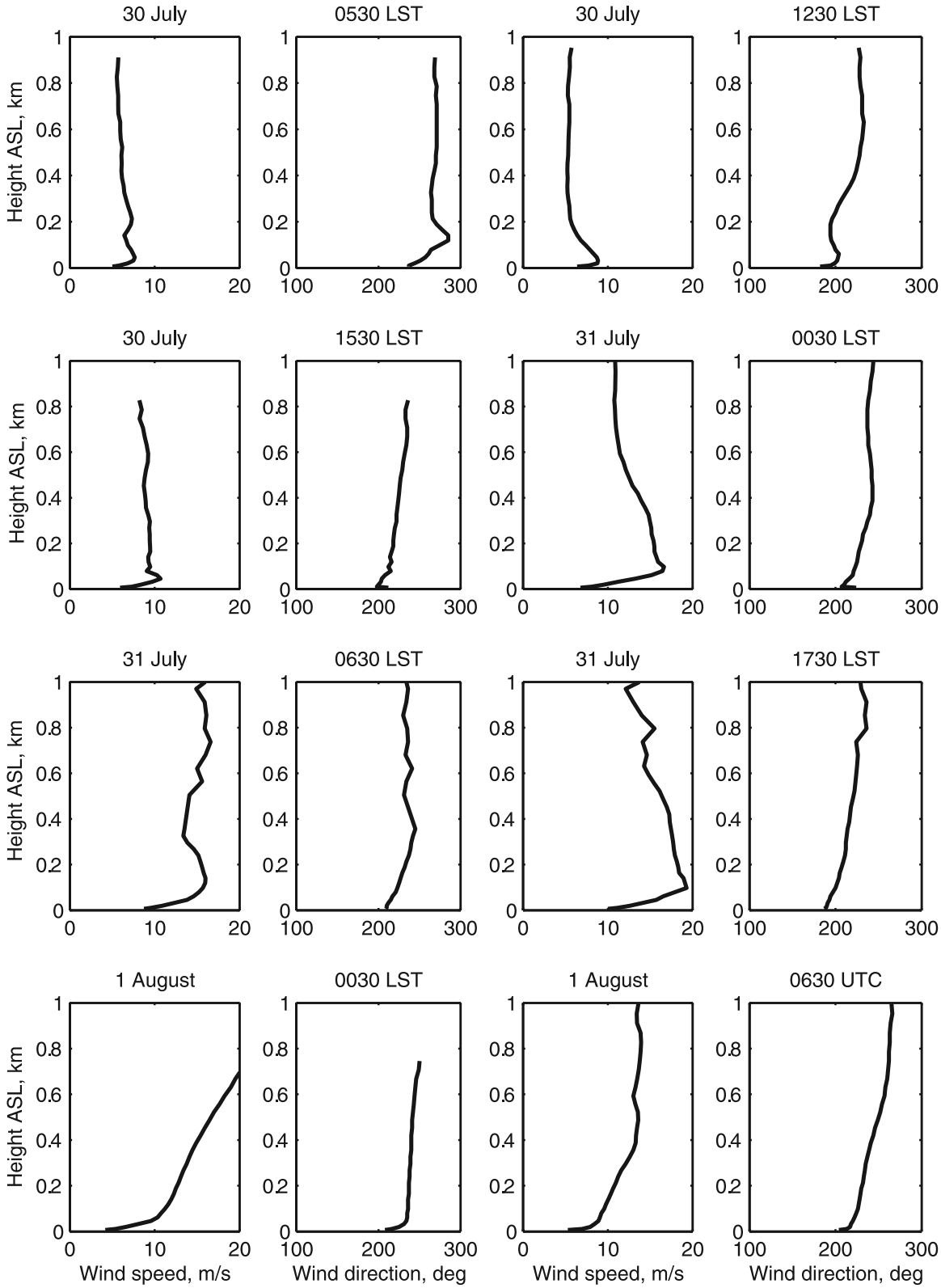

Figure 8. Wind speed and direction profiles at selected times during 30 July to 1 August.

some confidence. Figure 9a shows that (1) underpredicts the IBL height in most of the *Craig* [1946] cases, but performs reasonably well on average for the ICARTT cases. Figure 9b shows the normalized difference between prediction and measurement versus distance from shore. Perfect performance would produce a value of zero on the vertical axis. This makes clear that (1) underpredicts the IBL height for distances less than 20 km, but performs well or overpredicts

Table 1. Internal Boundary Layer Heights From *Craig* [1946] for Cases With Offshore Flow and Stable IBLs[a]

Case	Figure	Tsea	Theta_air	Wind, Beaufort	Wind Speed, m/s	x, km	h Measured	h Predicted	Measured – Predicted h	Measured – Predicted %
227	5	13	23	2	3	2.4	45	5	40	89
228	6	13	22	3	5.1	11.4	110	20	90	82
229	7	12	18	4	7.5	1.2	30	12	18	61
230	8	12	18	4	7.5	5.4	60	25	35	59
231	9	12	17	4	7.5	13.8	100	43	57	57
55	13	19	26	3	5.1	13.2	100	24	76	75
78	16	19	24	1	1.2	15	100	7	93	93
100	19	19	28	2	3	7.8	50	10	40	80
104	20	18	28	2	3	1.2	20	4	16	82
105	21	20	28	2	3	6.6	20	10	10	52
119	25	18	25	4	7.5	7.2	50	27	23	47
121	26	16	25	2	3	1.8	30	5	25	84
138	30	17	21	2	3	12	60	18	42	70
140	31	17	21	3	5.1	6	60	22	38	64
143	32	18	24	2	3	8.4	60	12	48	80
144	33	16	22	1	1.2	4.8	60	4	56	94
161	35	16	26	4	7.5	1.8	50	11	39	78

[a]The measured IBL height h is compared with values calculated from (1).

for longer distances. The cases at <20 km include the 15 and 16 July cases (section 2) at 10 km. There is some uncertainty in the leading constant in (1). A factor of 2 increase in that constant would fix the underprediction at 5–20 km distances, but at the cost of worsening the prediction at longer distances.

[17] The most likely source of the underprediction is that the derivation of (1) does not include advected turbulence [*Mahrt et al.*, 2001; *Vickers et al.*, 2001]. Briefly stated, the vigorous convective turbulence over land continues for a few eddy turnover times (20–30 min) after the surface heating (and therefore turbulence production) has been cut off by the air's passage over the shoreline. This decaying turbulence works against the increasing static stability to provide the mixing required to cool the layer. Because the ICARTT measurements were not closer to shore, we did not succeed in capturing the initial formation of the stable layer, and therefore did not succeed in directly answering our key question about how the stable BL is formed.

[18] At longer fetch the temperature profile approaches a state of equilibrium and the shape can be approximated with quasi-stationary forms (see *Garratt* [1992] for discussion). However, *Smedman et al.* [1997a] find that the boundary layer eventually evolves to a near-neutral surface layer with a shallow mixed layer above. This occurs at a fetch given by

$$x_{neut} = \left(\frac{75(\theta_v - \theta_{vs})}{\theta_v}\right)^2 \frac{U}{f}, \tag{2}$$

which is about 500 km for typical conditions during ICARTT. Such long fetch is well outside the domain of the ship measurements in ICARTT.

[19] Various classification schemes have been advanced for stable boundary layers. For example, *Mahrt et al.* [1998] set forth three categories: weakly stable, transition, and very stable. The classification is based on the stability parameter z/L, where z is the measurement height and L is the Obukhov length. During the 15–16 July period, the boundary layer at the ship was always very stable, with z/L greater than 1 (based on the inertial dissipation flux measurements). On 30 July to 1 August, the boundary layer was very stable early and late in the period. In the middle of the period, the boundary layer was in a transitional stability regime, with $0.1 < z/L < 1$.

Table 2. Data for Soundings From the *Ronald H. Brown*, Including Estimated Distances From Land for Air at the Surface[a]

Date	Time, LST	Latitude	Longitude	Tsea	Theta _air	Coast Latitude	Coast Longitude	x, km	Time, h	U (x/t), m s^{-1}	h	h Predicted
15 Jul	1800	42.74	−70.7	15.30	22.01			10	0.3	5.0	40	21
16 Jul	0600	42.74	−70.7	15.03	18.72			10	0.3	5.0	40	28
30 Jul	0600	42.59	−70.08	15.76	18.85	42.25	−70.67	61	4	4.2	37	65
30 Jul	1200	43.29	−70.52	17.66	20.65	42.74	−70.82	66	5	3.7	35	60
30 Jul	1500	43.29	−69.57	19.34	22.52	41.96	−70.58	169	14	3.4	75	85
30 Jul	0000	43.64	−69.65	13.35	22.53	41.78	−70.07	210	10	5.8	97	97
31 Jul	0600	43.64	−69.99	16.08	20.98	42.17	−70.64	172	8	6.0	107	123
31 Jul	1200	43.33	−70.32	17.79	24.97	42.01	−70.6	148	7	5.9	101	93
31 Jul	1800	43.13	−70.31	16.96	23.66	41.81	−70.44	147	5	8.2	46	133
1 Aug	0000	42.98	−70.63	16.37	23.63	42.76	−70.73	26	1	7.2	61	48
1 Aug	0600	42.98	−70.63	17.09	23.25	42.77	−70.81	28	1	7.8	67	58
1 Aug	1800	43.55	−70.11	14.88	24.77	42.44	−70.84	137	6	6.3	81	82

[a]IBL height h as measured and as predicted from (1) are shown.

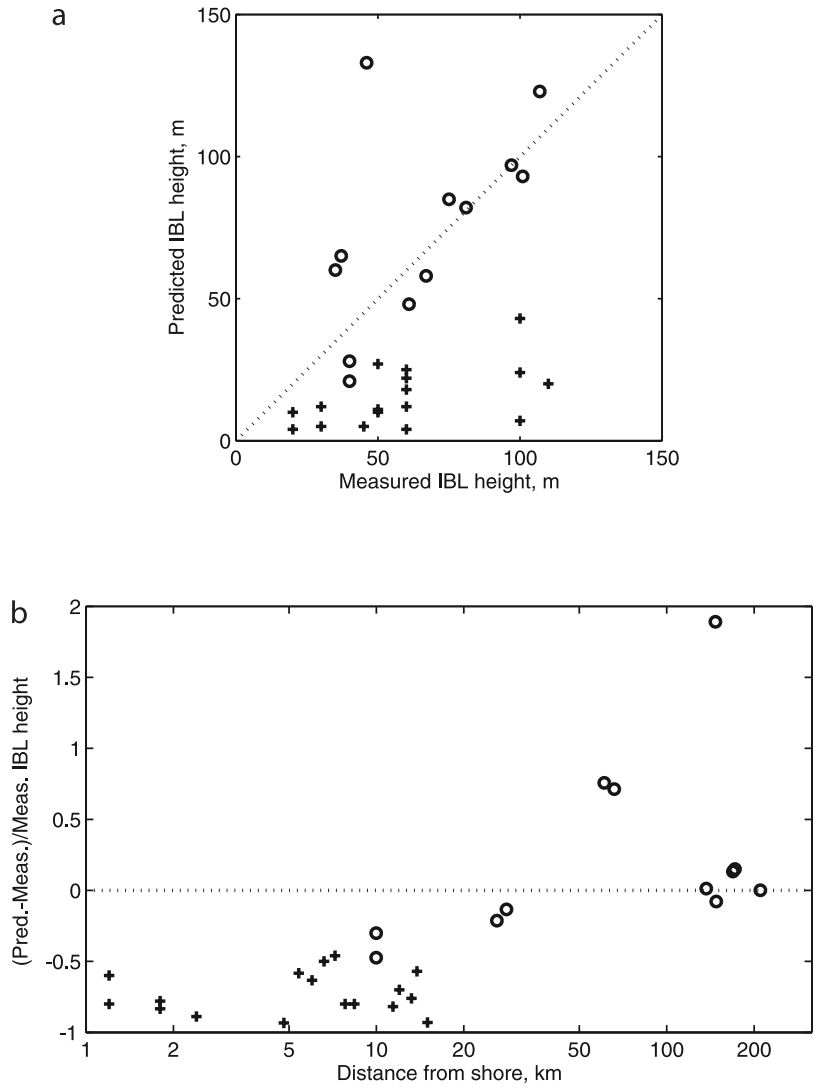

Figure 9. Comparisons of measured IBL heights from *Craig* [1946] (pluses) and ICARTT 15–16 July and 30 July to 1 August (circles). (a) A direct comparison of the measured and predicted heights. (b) Difference of the measured and predicted heights normalized by the measured height. In Figure 9b, the vertical axis is the difference between measurement and prediction divided by the measured value, and the horizontal axis is a logarithmic scale of distance from shore along a trajectory at the surface.

[20] According to the stability classification, the very stable boundary layer ($z/L > 1$) should be only intermittently turbulent. However, the boundary layers observed from the ship during these periods seem to be continuously (albeit weakly) turbulent. Richardson numbers (bulk or flux) calculated from the ship measurements are always less than 0.25, generally less than 0.1. In the absence of any clear guidance in the literature, we take 0.25 as a reasonable estimate of the critical value below which turbulence should be produced. It should also be noted that these boundary layers are shallow enough that there may be significant flux divergence between the surface and the measurement height [*Fairall et al.*, 2006]. This means that the measurements probably underestimate the magnitude of the surface heat flux. The effect on the computation of z/L is not clear, since both the stress (momentum flux) and heat flux are affected.

[21] Another perspective on stability classification is offered by *Mahrt and Vickers* [2005]. On the basis of vertical velocity variances, they define "weak" or "extremely weak" and "strong" turbulence regimes. Our 15–16 July nearshore data (Figure 2) have vertical velocity variances that fall within the weak regime. Our traditional processing using 10-min averaging times probably includes considerable influence from mesoscale motions [*Mahrt and Vickers*, 2005], so the true turbulence variances are probably even smaller. Our 30 July to 1 August data are again in an intermediate regime.

[22] Wind profiles observed over the Gulf of Maine commonly show substantial directional and vector shear between the surface and 100 m, and even greater directional shear between the surface and 500 m. Directional shear was less in the moderately stable regime (31 July) than in the

strongly stable regimes before and after, while vector shear between the surface and 100 m was greater in the moderately stable subperiod. The entire 15–16 July period was very stable, but the directional shear in the layer below 100 m was least when heat flux magnitude was greatest (even though the flux was small).

[23] According to theory, the evolution of one wind component is given by

$$\frac{DU}{Dt} = f\left(V - V_g\right) - \frac{\partial\left(\overline{w'u'}\right)}{\partial z} \tag{3}$$

where V_g is the geostrophic wind associated with the horizontal pressure gradient, F is the Coriolis parameter, and $\overline{w'u'}$ is the U-component turbulent stress (the ageostrophic component). Transitions to stable boundary layers are characterized by wind jets near the top of the boundary layer. The situation in coastal regions tends to be more complicated than that of the classic explanation for the nocturnal jet over land [*Blackadar*, 1957], for which case the daytime balance of the RHS of (3) is upset after sundown by reduction of the ageostrophic term associated with decreasing surface winds and reduced surface stress in a stable surface layer. Initially a jet forms along the mean wind direction and then rotates with period 1/f.

[24] However, the coastal region is characterized by horizontal variations that have implications for the geostrophic component [*Kaellstrand et al.*, 2000]. In the southern Gulf of Maine, the horizontal temperature gradient in the boundary layer is approximately east-west (warmer land to the west of cooler water) while the larger-scale temperature gradient, affecting the free troposphere, is north-south. The geostrophic term can be illuminated by taking a top-down view where we consider a synoptic-scale pressure gradient term, V_{go}, and a local thermal wind component confined to the boundary layer.

$$V_g(z) = V_{go} + \int_z^{h+} \frac{\partial V_g}{\partial z} dz \tag{4}$$

[25] The upper limit of this integral is just above the IBL. We can expand the integral as

$$V_g(z) = V_{go} + \frac{g}{f\theta_v}\Delta\theta_v \frac{\partial h}{\partial x} - \frac{g}{2f\theta_v}(h - z)\frac{\partial \theta_v}{\partial x} \tag{5}$$

where $\Delta\theta_v$ is the jump in θ_v across the inversion at h [*Fairall*, 1984]. From (5) it is clear that a west-to-east IBL would tend to produce a jet in the south-to-north component near the top of the IBL. For the conditions quoted above, the second term on the RHS of (5) yields a 3 m s^{-1} increase in the upper boundary layer.

[26] On the basis of data collected in the Arctic over pack ice during the SHEBA experiment, *Grachev et al.* [2005] identified several scaling regimes in the stable boundary layer (SBL) that are associated with different physical mechanisms. Different SBL regimes are described in terms of the Monin-Obukhov stability parameter (z/L), the Ekman number (Ek) that quantifies the influence of the Earth's rotation, and the bulk Richardson number (Ri_B) that determines the intensity of the turbulence. These three nondimensional parameters govern four major regimes. As stability increases, and the Richardson number approaches its critical value, the surface layer, where the turbulence is continuous, may be very shallow (less than 5 m). In this regime, the wind structure is influenced by the Coriolis force. Observed wind speeds show features of the Ekman spiral even near the surface (surface Ekman layer). The boundary layers in the Gulf of Maine, described in this paper, have been recently influenced by land, and are not expected to show the same Coriolis influence.

[27] Pollutant transport in this boundary layer cannot be modeled or understood without capturing the vertical structure in the winds. Modeling at 2.5 km grid spacing with a fine vertical grid captures some, but not all, of the important effects [*Angevine et al.*, 2006]. The model developed a stable boundary layer, but not as quickly (not as close to shore) as in reality, and the modeled layer was less stable and deeper than observed. The wind shear was also less than observed. If chemical transport is being modeled, the less stable boundary layer in a model may result in decreased isolation of the layers aloft from the surface, and therefore less efficient long-range transport than that described by *Neuman et al.* [2006]. *Skyllingstad et al.* [2005] did mesoscale and large-eddy simulation modeling studies for offshore flow onto cold water (5 K cooler than the incident boundary layer) and found turbulent kinetic energy and surface stress dropping rapidly within a few km of shore. Their results show the boundary layer cooled less than 1 K at 4 km fetch with a stable surface layer about 20 m thick. At 30 km downwind, cooling was modeled up to 100 m and the near-surface cooling was about 2 K. *Lapworth* [2005] considered the near-surface wind in warm flow over cool water with an air-sea temperature difference of 6 K from both observations and two-dimensional modeling.

[28] On a few occasions during the study, instruments aboard the NOAA WP-3 aircraft measured small but significant amounts of dimethyl sulfide (DMS) (C. Warneke, personal communication, 2006). DMS occurred at the lowest altitudes reached by the aircraft, between 170 and 300 m ASL. DMS is produced at the sea surface by biological activity and has a fairly short lifetime, so these enhanced DMS levels suggest that there was some exchange between the atmosphere above 170 m and the sea surface. The exchange timescale in these cases must be a few hours or less.

[29] One period was a notable exception to the general rule of stable boundary layers over the water. On 8 August, a sounding at 0600 LST (not shown) showed a shallow convective boundary layer. At the time, the ship was just north of the tip of Cape Cod, and the flow at the ship was from the west (offshore). The traces of sea surface temperature and air temperature at the ship (not shown) show two periods when the water was warmer than the air, roughly 0220–0440 LST and 0550–0740 LST. The air temperatures are typical for nighttime over the nearby land, and the water temperatures are near the top of the range observed during the cruise. Even so, the observed convective boundary layer is shallow (~300 m) relative to typical daytime convective boundary layers over land (~1500–2000 m) and comparable to typical nocturnal boundary layer depths over land.

[30] Few or no clouds were present during the periods discussed here. During other periods of the ICARTT study, low clouds and fog were common. Fog and low clouds occurred primarily when the flow was not from the U.S. east coast. The boundary layer structure under those conditions is likely to be quite different than that described here.

[31] **Acknowledgments.** The authors thank all of the participants in ICARTT/NEAQS 2004 who aided in the operation of these instruments and the collection of data. A special thanks goes to the officers and crew of the NOAA Research Vessel *Ronald H. Brown* who provided not only scientific support but a friendly environment in which to work. This work was supported by the NOAA Health of the Atmosphere program, the NOAA Carbon Cycle program, and the NOAA ESRL Physical Sciences Division Director's Fund.

References

Angevine, W. M., et al. (2004), Coastal boundary layer influence on pollutant transport in New England, *J. Appl. Meteorol.*, *43*, 1425–1437.

Angevine, W. M., M. Tjernstrom, and M. Zagar (2006), Modeling of the coastal boundary layer and pollutant transport in New England, *J. Appl. Meteorol. Climatol.*, *45*, 137–154.

Atkinson, B. W., and M. Zhu (2005), Radar-duct and boundary-layer characteristics over the area of the Gulf, *Q. J. R. Meteorol. Soc.*, *131*, 1923–1953.

Atkinson, B. W., J.-G. Li, and R. S. Plant (2001), Numerical modeling of the propagation environment in the atmospheric boundary layer over the Persian Gulf, *J. Appl. Meteorol.*, *40*, 586–603.

Blackadar, A. K. (1957), Boundary layer wind maxima and their significance for the growth of nocturnal inversions, *Bull. Am. Meteorol. Soc.*, *38*, 283–290.

Brooks, I. M., and D. P. Rogers (2000), Aircraft observations of the mean and turbulent structure of a shallow boundary layer over the Persian Gulf, *Boundary Layer Meteorol.*, *95*, 189–210.

Brooks, I. M., A. K. Goroch, and D. P. Rogers (1999), Observations of strong surface radar ducts over the Persian Gulf, *J. Appl. Meteorol.*, *38*, 1293–1310.

Chimonas, G. (2005), The nighttime accelerations of the wind in the boundary layer, *Boundary Layer Meteorol.*, *116*, 519–531.

Craig, R. A. (1946), Measurements of temperature and humidity in the lowest 1000 feet of the atmosphere over Massachusetts Bay, *Pap. Phys. Oceanogr. Meteorol.*, *10*, 1–47.

Emmons, G. (1947), Vertical distributions of temperature and humidity over the ocean between Nantucket and New Jersey, *Pap. Phys. Oceanogr. Meteorol.*, *10*, 1–89.

Fairall, C. W. (1984), Wind shear enhancement of entrainment and refractive index structure parameter at the top of a turbulent mixed layer, *J. Atmos. Sci.*, *41*, 3472–3484.

Fairall, C. W., L. Bariteau, A. A. Grachev, R. J. Hill, D. E. Wolfe, W. A. Brewer, S. C. Tucker, J. E. Hare, and W. M. Angevine (2006), Turbulent bulk transfer coefficients and ozone deposition velocity in the International Consortium for Atmospheric Research into Transport and Transformation, *J. Geophys. Res.*, doi:10.1029/2006JD007597, in press.

Garratt, J. R. (1990), The internal boundary layer—A review, *Boundary Layer Meteorol.*, *50*, 171–203.

Garratt, J. R. (1992), *The Atmospheric Boundary Layer*, 316 pp., Cambridge Univ. Press, New York.

Grachev, A. A., C. W. Fairall, P. O. G. Persson, E. L. Andreas, and P. S. Guest (2005), Stable boundary-layer scaling regimes: The SHEBA data, *Boundary Layer Meteorol.*, *116*, 201–235.

Kaellstrand, B., H. Bergstroem, J. Hoejstrup, and A.-S. Smedman (2000), Mesoscale wind field modifications over the Baltic Sea, *Boundary Layer Meteorol.*, *95*, 161–188.

Lapworth, A. J. (2005), The diurnal variation of the marine surface wind in an offshore flow, *Q. J. R. Meteorol. Soc.*, *131*, 2367–2387.

Lundquist, J. K. (2003), Intermittent and elliptical inertial oscillations in the atmospheric boundary layer, *J. Atmos. Sci.*, *60*, 2661–2673.

Mahrt, L., and D. Vickers (2005), Extremely weak mixing in stable conditions, *Boundary Layer Meteorol.*, *119*, 19–39, doi:10.1007/s10546-10005-19017-10545.

Mahrt, L., J. Sun, W. Blumen, A. C. Delany, and S. Oncley (1998), Nocturnal boundary-layer regimes, *Boundary Layer Meteorol.*, *88*, 255–278.

Mahrt, L., D. Vickers, J. Sun, T. L. Crawford, G. Crescenti, and P. Frederickson (2001), Surface stress in offshore flow and quasi-frictional decoupling, *J. Geophys. Res.*, *106*, 20,629–20,639.

Neuman, J. A., et al. (2006), Reactive nitrogen transport and photochemistry in urban plumes over the North Atlantic Ocean, *J. Geophys. Res.*, *111*, D23S54, doi:10.1029/2005JD007010.

Rogers, D. P., D. W. Johnson, and C. A. Friehe (1995), The stable internal boundary layer over a coastal sea. Part I: Airborne measurements of the mean and turbulence structure, *J. Atmos. Sci.*, *52*, 667–683.

Skyllingstad, E. D., R. M. Samelson, L. Mahrt, and P. Barbour (2005), A numerical modeling study of warm offshore flow over cool water, *Mon. Weather Rev.*, *133*, 345–361.

Smedman, A.-S., H. Bergstroem, and B. Grisogono (1997a), Evolution of stable internal boundary layers over a cold sea, *J. Geophys. Res.*, *102*, 1091–1099.

Smedman, A.-S., U. Hoegstroem, and H. Bergstroem (1997b), The turbulence regime of a very stable marine airflow with quasi-frictional decoupling, *J. Geophys. Res.*, *102*, 21,049–21,059.

Vickers, D., L. Mahrt, J. Sun, and T. L. Crawford (2001), Structure of offshore flow, *Mon. Weather Rev.*, *129*, 1251–1258.

White, A. B., C. J. Senff, A. N. Keane, L. S. Darby, I. V. Djalalova, D. C. Ruffieux, D. E. White, B. J. Williams, and A. H. Goldstein (2006), A wind profiler trajectory tool for air-quality transport applications, *J. Geophys. Res.*, doi:10.1029/2006JD007475, in press.

Zhu, M., and B. W. Atkinson (2005), Simulated climatology of atmospheric ducts over the Persian Gulf, *Boundary Layer Meteorol.*, *115*, 433–452.

W. M. Angevine, W. A. Brewer, C. W. Fairall, J. E. Hare, R. J. Hill, A. B. White, and D. E. Wolfe, NOAA ESRL R/CSD04, 325 Broadway, Boulder, CO 80305-3337, USA. (wayne.m.angevine@noaa.gov)